Alteration of Conformation and Dynamics of Bacteriorhodopsin Induced by Protonation of Asp 85 and Deprotonation of Schiff Base as Studied by ^{13}C NMR†

Yasuharu Kawase,‡ Michikazu Tanio,‡ Atushi Kira,‡ Satoru Yamaguchi,‡ Satoru Tuzi,‡ Akira Naito,‡ Mikio Kataoka,§ J. K. Lanyi,|| R. Needleman,⊥ and Hazime Saitô*,‡

Department of Life Science, Faculty of Science, Himeji Institute of Technology, Harima Science Garden City, Kouto 3-chome, Kamigori, Hyogo, Japan 678-1297, Department of Material Science, Nara Institute of Science and Technology, Ikoma, Nara, Japan, 630-0101, Department of Biophysics and Physiology, University of California, Irvine, California 92697-4560, and Department of Biochemistry, Wayne State University, Detroit, Michigan 48201

Received July 7, 2000; Revised Manuscript Received August 22, 2000

ABSTRACT: According to previous X-ray diffraction studies, the D85N mutant of bacteriorhodopsin (bR) with unprotonated Schiff base assumes a protein conformation similar to that in the M photointermediate. We recorded ^{13}C NMR spectra of [3-^{13}C]Ala- and [1-^{13}C]Val-labeled D85N and D85N/D96N mutants at ambient temperature to examine how conformation and dynamics of the protein backbone are altered when the Schiff base is protonated (at pH 7) and unprotonated (at pH 10). Most notably, we found that the peak intensities of three to four [3-^{13}C]Ala-labeled residues from the transmembrane α-helices, including Ala 39, 51, and 53 (helix B) and 215 (helix G), were suppressed in D85N and D85N/D96N both from CP-MAS (cross polarization-magic angle spinning) and DD-MAS (dipolar decoupled-magic angle spinning) spectra, irrespective of the pH. This is due to conformational change and subsequent acquisition of intermediate time-range motions, with correlation times in the order of 10^{-5} or 10^{-4} s, which interferes with proton decoupling frequency or frequency of magic angle spinning, respectively, essential for an attempted peak-narrowing to achieve high-resolution NMR signals. Greater changes were achieved, however, at pH 10, which indicate large-amplitude motions of transmembrane helices upon deprotonation of Schiff base and the formation of the M-like state in the absence of illumination. The spectra detected more rapid motions in the extracellular and/or cytoplasmic loops, with correlation times increasing from 10^{-4} to 10^{-5} s. Conformational changes in the transmembrane helices were located at helices B, G, and D as viewed from the above-mentioned spectral changes, as well as at 1-^{13}C-labeled Val 49 (helix B), 69 (B−C loop), and [3-^{13}C]Ala-labeled Ala 126 (D-helix) signals, in addition to the cytoplasmic and extracellular loops. Further, we found that in the M-like state the charged state of Asp 96 at the cytoplasmic side substantially modulated the conformation and dynamics of the extracellular region through long-distance interaction.

Bacteriorhodopsin (bR)[1] is a light-driven proton pump in the purple membrane of *Halobacterium salinarum*, consisting of seven transmembrane α-helices, A to G, linked to the chromophore, retinal, at Lys 216. The three-dimensional structure of bR in the unphotolyzed state has been determined by cryo-electron microscopy of tilted two-dimensional crystals (*1*−*3*) and X-ray diffraction of three-dimensional crystals (*4*−*8*), although the conformation of interfacial residues such as loops are not always consistent in these reports. Photoisomerization of the retinal from the all-trans to 13-cis form initiates proton-transfer steps from the cytoplasmic to the extracellular side via the J, K, L, M, N, and O intermediates of a cyclic reaction. Global conformational changes of the protein backbone occur in the M and/or N intermediates with deprotonated and reprotonated retinal Schiff base, respectively, as observed with neutron (*9*, *10*), X-ray (*11*−*14*), and electron diffraction (*15*−*17*). Tertiary structural changes may occur between the M states (M_1 and M_2 states) as well (*14*). Such global conformational changes may be part of the proton access switch between the deprotonation and reprotonation of the Schiff base (*18*−*20*).

One report maintained that the characteristic conformational changes of the M intermediate are at helices B and G and the change of the N intermediate is at helices F and G (*21*), while another concluded that the conformations of M and N are essentially the same (*16*). The movement of helix F was proposed to open a channel to transport a proton from the cytoplasmic surface (*15*, *22*). These movements of the transmembrane helices are characterized by large-amplitude movements of the C−D and E−F loops, as detected by site-directed EPR spectroscopy (*22*−*25*). Luecke et al. (*26*) recently showed that in three-dimensional crystals this kind

† This work was partially supported by Grants-in-Aids for Scientific Research from the Ministry of Education, Science, Sports and Culture of Japan (09480179, 10044092).

* To whom corresponding should be addressed. Phone: +81-791-58-0181. Fax: +81-791-58-0182. E-mail: saito@sci.himeji-tech.ac.jp.
‡ Himeji Institute of Technology.
§ Nara Institute of Science and Technology.
|| University of California, Irvine.
⊥ Wayne State University.

[1] Abbreviations: AFM, atomic force microscope; bR, bacteriorhodopsin; CP-MAS, cross polarization-magic angle spinning; DD-MAS, dipolar decoupled- magic angle spinning; EPR, electron paramagnetic resonance; FTIR, Fourier transform infrared spectroscopy; TMS, tetramethylsilane; WT, wild-type.

10.1021/bi0015820 CCC: $19.00
Published on Web 11/03/2000

of structural change in helices F and G resulted in the severe disordering of regions that are ordered in bR state rather than discrete conformational changes. It is worthwhile therefore to characterize the backbone dynamics in more detail by spectroscopic means, because no information is available from diffraction studies as to the nature and time-scale of the conformational fluctuations in such systems, as they could play important roles in initiating various kinds of biologically important processes.

Several approaches have been made to trap the M state, by illuminating wild-type bR either at a temperature between 220 and 260 K (*27*) or in the presence of guanidium hydrochloride at pH 9.6 (*9*, *12*). An M-like state was demonstrated to arise for D85N mutant without illumination (*18*), because the lowered pK_a of Schiff base allows its deprotonation at alkaline condition (pH ~10) at ambient temperature (*28*−*30*), and the global conformation is apparently destabilized by loss of interaction of the positively charged Schiff base with the neighboring anionic residues. This system, together with the double mutant D85N/D96N, was extensively studied (*18*, *31*) to analyze the two conformations labeled as conformations C and E, in which access of Schiff base proton was postulated to be to the cytoplasmic and the extracellular side, respectively. To further characterize this conformation equilibrium, it will be important to utilize nonperturbing probes at ambient temperature. Spin- or heavy-atom labeling techniques (*22*−*25*, *32*−*34*) are not necessarily free of perturbation from the labels.

As an alternative, ^{13}C NMR approach has proved to be excellent nonperturbing means, especially at ambient temperature, for probing conformation and dynamics of [3-^{13}C]-Ala- or [1-^{13}C]Val-labeled bR (*35*−*45*). This approach is based mainly on the conformation-dependent displacement of ^{13}C chemical shifts, which vary quite sensitively with the local conformation (up to 8 ppm), and for reference utilizes data from model polypeptides whose secondary structures are well characterized (*45*−*48*). It should be recognized, however, that *such NMR signals are not always detectable from all regions of membrane proteins at ambient temperature in physiologically important, fully hydrated preparations*, because the protein backbone is not always rigid but can undergo a variety of local conformational fluctuations on various time scales, resulting in peak-suppression for specific residues. Taking advantage of this, one can utilize the ^{13}C NMR approach to distinguish the following three types of motions: (i) fast isotropic or large-amplitude motions which facilitate averaging of dipolar interactions (with correlation time shorter than 10^{-8} s), (ii) intermediate (with correlation time in the order of 10^{-5} s), and (iii) slow motions with correlation times in the order of 10^{-4} s which are related to suppression of ^{13}C NMR signals from CP-MAS (cross polarization−magic angle spinning) alone due to reduced CP efficiency (*49*), or in both CP-MAS and DD-MAS (dipolar decoupled−magic angle spinning) spectra due to interference of motions with proton decoupling frequency or magic angle spinning (*50*).

In this work, we report on ^{13}C NMR spectra of [3-^{13}C]-Ala- or [1-^{13}C]Val-labeled D85N and D85N/D96N mutants at alkaline pH, with the Schiff base deprotonated and a resultant structural change very similar to that of the M photointermediate (*18*, *30*). This change occurs without illumination, at *ambient temperature*. We found that the acquisition of intermediate motion with correlation time of 10^{-5} s is achieved in the transmembrane helices irrespective of their pH, and further suppression of several transmembrane α-helical peaks and interhelical loops caused by deprotonated state of Schiff base in both mutants (pH 10). In the former, conformational changes both at the vicinity of Val 49 (helix B), 69 (B−C loop), and Ala 126 (see Figure 1 for the primary sequence and schematic representation of secondary structure based on X-ray diffraction study) were also identified in view of specific displacements of ^{13}C chemical shifts of [1-^{13}C]-Val- and [3-^{13}C]Ala-labeled D85N mutant, respectively, at pH 10. Nevertheless, distinct change in the conformation and dynamics in the extracellular side was noteworthy between D85N and D85N/D96N mutants at pH 10 at the deprotonated state of Schiff base: acquisition of accelerated motions to the order of 10^{-5} s for both the cytoplasmic and extracellular loops in the former, while such motion is present only at the cytoplasmic side in the latter. This finding is the direct evidence for the presence of long-distance interactions to show that the charged state of Asp 96 at the cytoplasmic side regulates the conformation and dynamics of the extracelluar side also.

MATERIALS AND METHODS

[3-^{13}C]Ala- and [1-^{13}C]Val-labeled preparations were obtained by growing the S9 strain (wild-type) *of Halobacterium salinarum* and D85N, D96N, and D85N/D96N mutants in the TS medium of Onishi et al. (*51*) in which unlabeled L-alanine or L-valine was replaced with the corresponding ^{13}C-labeled amino acids under consideration. Purple or blue membranes containing bR or mutants were isolated by the method of Oesterhelt and Stoeckenius (*52*) and concentrated by centrifugation at 39800*g* for 1.5 h, followed by suspension in 5 mM HEPES (pH 7.0) buffer containing 10 mM NaCl and 0.025% NaN_3. Proteolysis of D85N by papain was performed by the method of Liao and Khorana (*53*), and its purity was checked by SDS−PAGE gel electrophoresis. For NMR measurements of [3-^{13}C]Ala-labeled proteins at higher pH (pH 8, 10, and 11), the bR or D85N preparations were suspended in either 20 mM CHES (pH 8 and 10) or 20 mM CAPS (pH 11) buffer containing 10 mM NaCl and 0.025% NaN_3. [1-^{13}C]Val- and [3-^{13}C]Ala-D85N/D96N and [1-^{13}C]-Val-D85N were therefore suspended in mixed buffer containing 5 mM of each MES, HEPES, TAPS, CHES, and CAPSP, and 10 mM NaCl and 0.025% NaN_3. Suspended pellets in such buffer were placed into a 5-mm o.d. zirconia pencil-type rotor for the magic angle spinning NMR, and the rotor was tightly sealed with Teflon caps with rapid Araldyte to prevent leakage or evaporation of water from the samples during magic angle spinning at 2.6 and 4 kHz, under stream of compressed dried air, for recording ^{13}C NMR spectra of [3-^{13}C]Ala- and [1-^{13}C]Val-labeled proteins, respectively.

High-resolution solid-state ^{13}C NMR spectra (100.6 MHz) were recorded on a Chemagnetics CMX-400 solid-state NMR spectrometer by CP-MAS and DD-MAS with single pulse excitation techniques. ^{13}C NMR spectra were recorded mainly at ambient temperature (20 °C) under dark condition. The $\pi/2$ pulses for ^{13}C and ^{1}H nuclei were 4.5−5 μs. The spectral width and contact, repetition, and acquisition times for CP-MAS NMR experiments were 40 kHz, 1 ms, 4 s and 50 ms, respectively. Free induction decays (FIDs) were

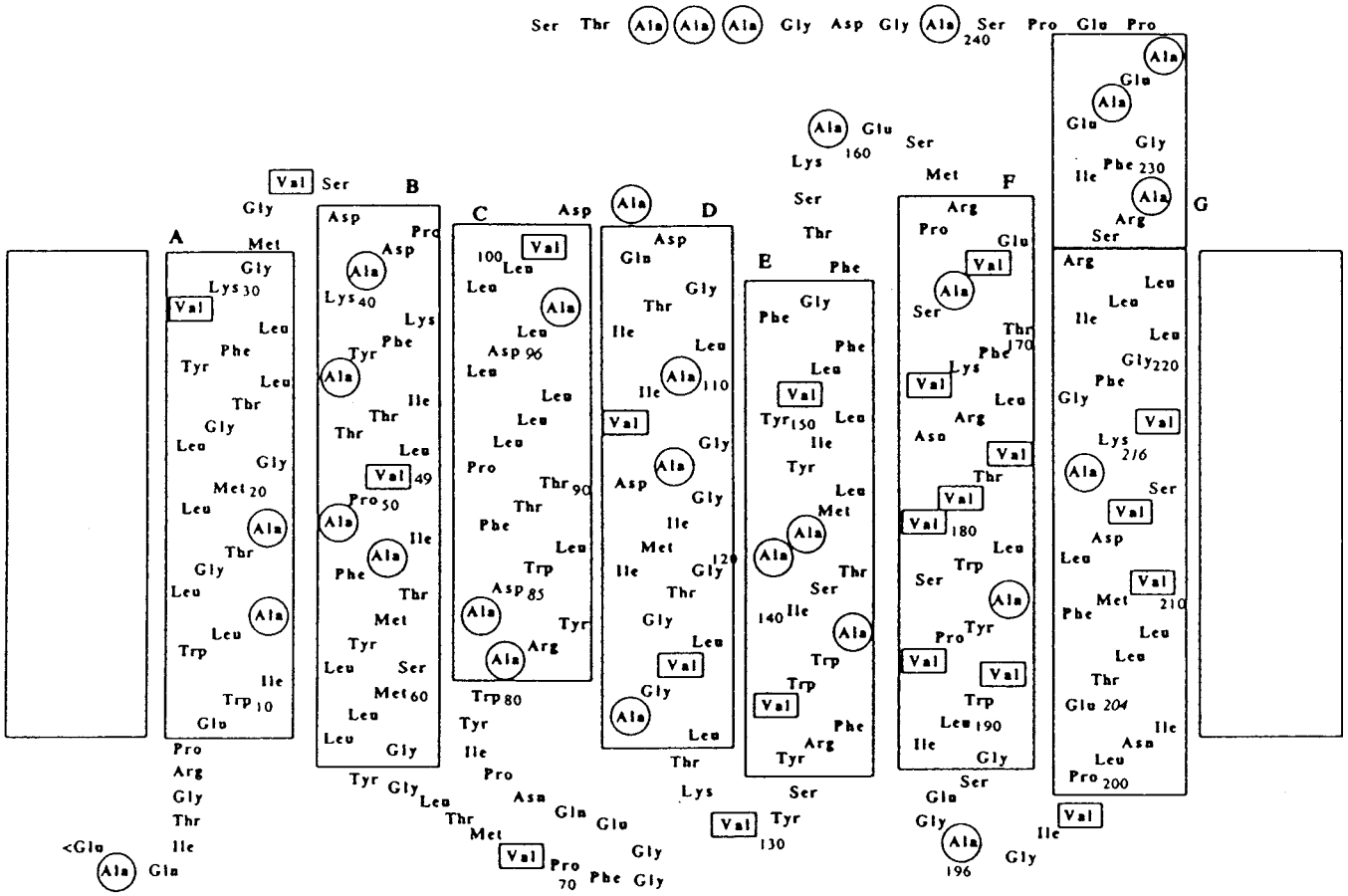

FIGURE 1: Schematic representation of the primary and secondary structure of bR based on X-ray diffraction study (*6*). Ala and Val residues labeled by [3-^{13}C]alanine and [1-^{13}C]valine were indicated by the circles and boxes, respectively.

acquired with 2K data points and Fourier transformed as 16K data points after 14K data points were zero-filled to improve the digital spectral resolution. A resolution enhancement was performed by the method of Gaussian multiplication. A typical parameter, 20 Hz for GB, was used for recording the ^{13}C NMR spectra of [3-^{13}C]Ala-bR and 30 and 10 Hz for GB and LB, respectively were used for recording spectra of [1-^{13}C]Val-bR. ^{13}C chemical shifts were first referred to the carboxyl carbon signal of crystalline glycine (176.03 ppm from tetramethylsilane (TMS) and converted to the data from TMS.

RESULTS

We had reported earlier that the ^{13}C NMR spectrum of [1-^{13}C]Val-D85N was substantially altered from that of wild-type even at neutral pH (*41*). Here, the assignment of the peaks for D85N and wild-type was previously performed based on comparison of the ^{13}C NMR spectra between the wild-type and site-directed mutants, Mn^{2+} binding and enzymatic cleavage, as summarized already (*44*). The apparently low intensity peak at 16.34 ppm in D85N mutant at neutral pH (Figure 2A) arose from the peak-suppression of the intense two ^{13}C NMR signals at 16.41 (including Ala 39) and 16.19 ppm (including Ala 215) of wild-type (see Figure 4A) (*42*). This kind of spectral change may be caused mainly by loss of peaks due to interference of motions arising from conformational fluctuation, with time scale of 10^{-5} s with proton-decoupling frequency (*50*). Concomitant with the above-mentioned spectral changes in the transmembrane helices, significant spectral changes were noted in the loop

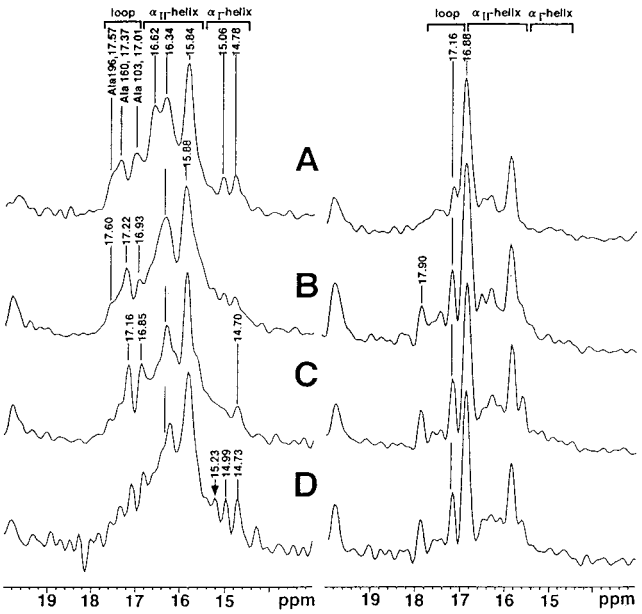

FIGURE 2: ^{13}C CP-MAS (left) and DD-MAS (right) NMR spectra of [3-^{13}C]Ala-labeled D85N mutant at various pH (7−11). Regio-specific assignment of peaks is give at the top trace. pH: (A), 7; (B), 8; (C), 10; (D), 11. The newly emerged peak at pH 11 is indicated by the arrow.

region also: the peak-position of Ala 196 signal of D85N, located at the F−G interhelical loop, was shifted upfield by 0.19 ppm, from 17.78 ppm of wild-type to 17.57 ppm of D85N mutant at neutral pH, while that of Ala 126 signal

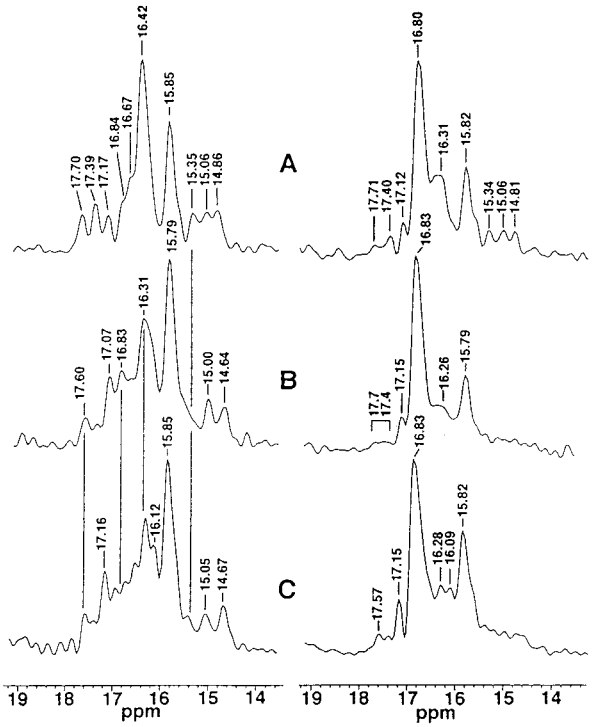

FIGURE 3: ^{13}C CP-MAS (left) and DD-MAS (right) NMR spectra of [3-^{13}C]Ala-labeled D96N at pH 7(A) and D85N/D96N (B and C) recorded at pH 7 and 10, respectively.

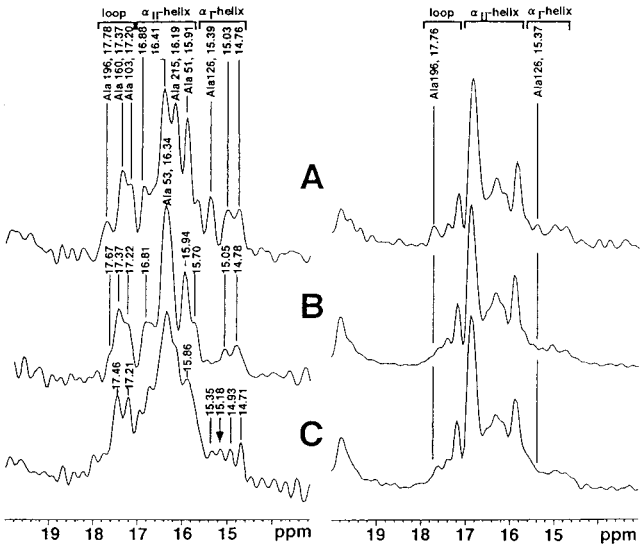

FIGURE 4: ^{13}C CP-MAS (left) and DD-MAS (right) NMR spectra of [3-^{13}C]Ala-wild-type at various pH (7−11). pH: (A) 7; (B) 10; (C) 11. The newly emerged peak at pH 11 is indicated by the arrow.

(15.39 ppm in the wild-type, see Figure 3A) at the extracelluar turn of helix D is displaced downfield in D85N (*42*). A minor conformational change at the F−G loop was noted already in the [1-^{13}C]Val-D85N mutant at neutral pH (*41*).

In addition to the above-mentioned changes, further reduction of the peak-intensity at 16.62 ppm (one or two Alas) was obtained in D85N upon raising the pH from 7 to 10 to deprotonate the Schiff base, at 16.34 (including Ala 53), 16.41 (including Ala 39), 16.19 (including Ala 215), and 15.96 and (including Ala 51). Such changes will have arisen from the M-like intermediate adopting the C-conformation (*18*), in view of the dynamical changes ascribable to residues located at helices B and G (Figure 2, spectra B−D). At higher pH, a more pronounced change is noted in the ^{13}C NMR spectra of the loop region also. Raising pH of the D85N mutant from 7 to 8 results in the gradual suppression of the two peaks of Ala 196 (17.57) and 160 (17.37), although the peak resonating at 17.22 (pH 8) and 17.16 ppm (pH 10) ascribable to Ala 103 remains almost unchanged. At pH 11, the S/N ratio of the ^{13}C CP-MAS NMR spectrum is considerably deteriorated because of the lowered efficiency of cross-polarization, although the corresponding DD-MAS spectrum is not. In the high-field region, only a signal at 14.70 ppm is visible at pH 10 (Figure 1C), despite the presence of the two peaks at 15.06 and 14.78 ppm at neutral pH. In addition, it is noteworthy that the intense new peak appeared at 17.90 ppm at pH 8−11 in the DD-MAS NMR spectra, although there is no such a peak in the CP-MAS NMR spectra.

In Figure 3, we compare ^{13}C CP-MAS (left) and DD-MAS (right) NMR spectra of [3-^{13}C]Ala-labeled D85N/D96N (B and C at pH 7 and 10, respectively) with those of D96N at pH 7(A). Obviously, the intense peak of wild-type at 16.19 ppm, including the signal of Ala 215 of helix G, is missing from D96N mutant. Importantly, the general profile of D85N/D96N is almost the same between the spectra recorded at pH 7 and 10 and very similar to those of D85N at high pH, consistent with the data by Kataoka et al. (*18*) which indicated that in the double-mutant the M-like state dominates even at pH 7, while in D85N it was detected only at pH 10. The exceptions to this were the downfield displacement of the peak from 17.07 to 17.16 ppm, the absence of the peak at 17.39 ppm and recovery of the peak at 15.35 ppm (Ala 126) by raising the pH. In both cases, the α_{II} peak at 16.19 ppm of wild-type is completely absent in D96N and D85N, but partially visible in D85N/D96N mutant as unresolved shoulder or resolved peak at 16.12 ppm. This means that the flexibility of the extracellular surface of the D85N mutant acquired upon deprotonation of Schiff base is not retained in the D85N/D96N mutant. In addition, the peak that resonated at 17.90 ppm, visible by the DD-MAS NMR in the D85N mutant is absent in the D85N/D96N double mutant at pH 10.

As the reference to the above-mentioned spectral changes of D85N and D85N/D96N mutants, we repeated these experiments with wild-type bR at alkaline pH, as illustrated in Figure 4, panels B and C. In general, the above-mentioned spectral changes are less pronounced in the wild-type but the decreased peak-intensity at 16.19 ppm assigned to Ala 215 [one or two Ala residue(s)] of the CP-MAS NMR spectrum is easily recognized at alkaline pH, although this peak is unchanged in the DD-MAS NMR spectra. More interestingly, the Ala 196 peak of the CP-MAS NMR spectrum (17.78 ppm) was suppressed at elevated pH at 11 as in D85N, indicating the decreased efficiency of cross polarization due to acquisition of fast large-amplitude motions, because this peak is visible in the DD-MAS NMR experiment. Likewise, it appears that the Ala 126 peak of wild-type is suppressed at pH 8, both in the CP-MAS and DD-MAS NMR spectra, due to interference with proton decoupling frequency (Figure 3B, right-handed trace). Again, the four peaks emerged at pH 11 in the α_I-helix, including the new peak indicated by an arrow at 15.18 ppm. It is also pointed out here that in the wild-type the large decrease of the 16.34 ppm (in D85N) does not occur, and instead it is

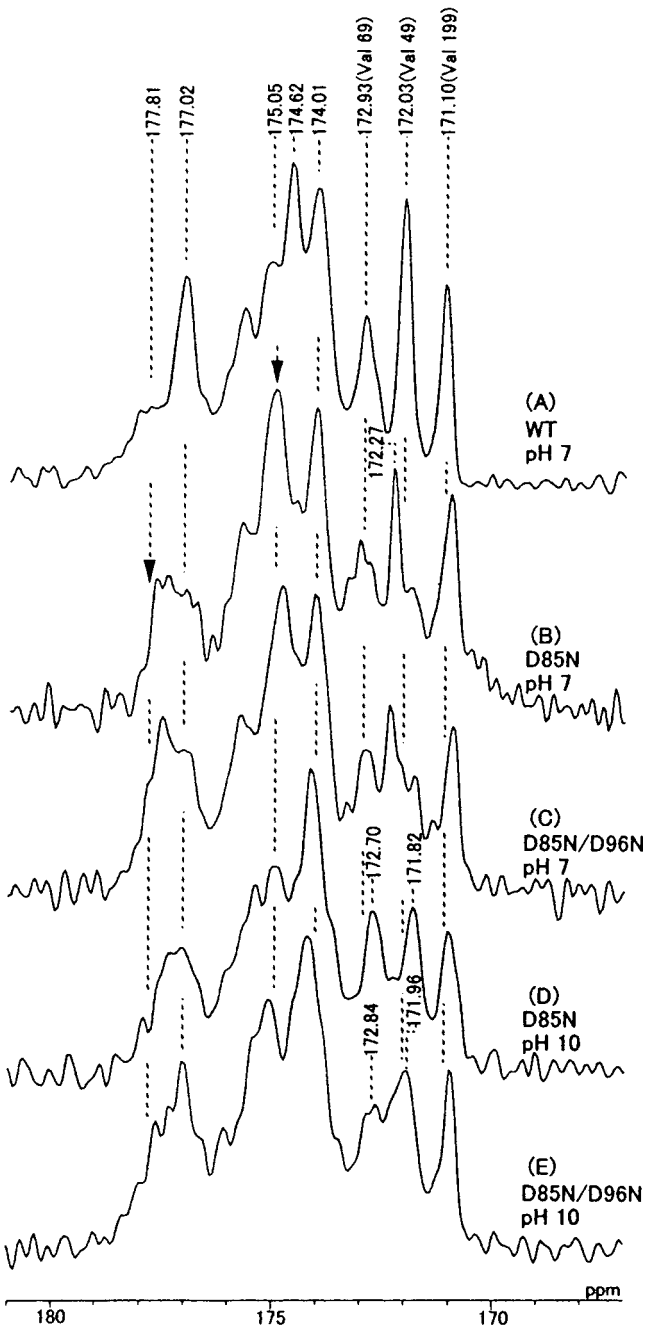

FIGURE 5: ^{13}C CP-MAS NMR spectra of [1-^{13}C]Val-labeled wild-type (A), D85N (B and D), and D85N/D96N (C and E) mutants recorded at pH 7 and 10.

the 15.91 ppm that is decreasing with pH 10. This means that no drastic motions, as in D85N and D85N/D96N mutants, are induced in the wild-type even at this high pH.

Figure 5 compares the ^{13}C NMR spectra of [1-^{13}C]Val-labeled D85N and D85N/D96N mutants both at pH 7 and 10 with reference to that of wild-type, to clarify how the above-mentioned spectral changes in the [3-^{13}C]Ala-labeled proteins (Figures 2-4) can be characterized as changes in the backbone dynamics. We assigned previously the well-resolved signals at 172.93, 172.03, and 171.10 ppm to [1-^{13}C]-Val 69, Val 49, and Val 199, respectively, on the basis of the spectral changes in the V49A, V199A mutants and specific cleavage by chymotrypsin (*41*). In contrast to the spectral changes in Figures 2 and 3, the ^{13}C NMR spectra of [1-^{13}C]Val-labeled D85N and D85N/D96N exhibited

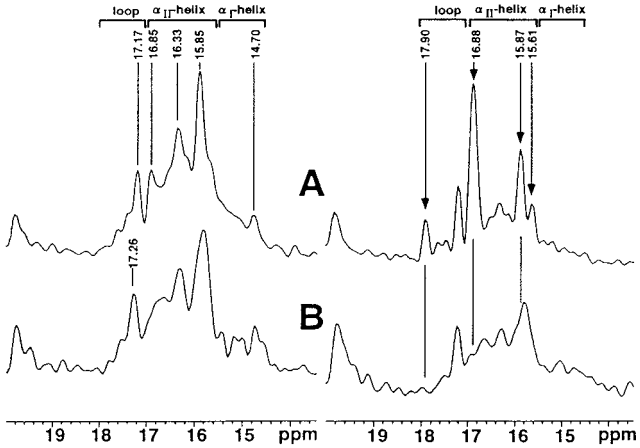

FIGURE 6: ^{13}C CP MAS (left) and DD-MAS (right) NMR spectra of [3-^{13}C]Ala-labeled D85N at pH 10 (A) and its papain-cleaved preparation (B). The peaks indicated by the arrows are ascribed to Ala residues located at the C-terminal protruded from the membrane surface.

almost the same spectral changes depending upon their respective pH, as compared with those of wild-type at pH 7. It is rather surprising to note, however, that the spectral pattern of D85N/D96N mutant at pH 10 is very similar to that of D85N at pH 9 (data not shown) despite the decreased pK_a of Schiff base in the double mutant relative to that of D85N (*18*). The three kinds of the ^{13}C NMR peaks (corresponding to the peak-intensity of at least single carbon), Val 49 (172.03 ppm), and two unassigned peaks 174.62 and 177.02 ppm, are displaced downfield with reference to those of wild-type by 0.24, 0.43, and 0.79 ppm, respectively, at pH 7 due to the neutralization of the electric charge at Asp 85. The lowermost peak at 177.81 ppm of D85N marked by the arrow was previously ascribed to a background signal (hatched peak) (*42*) but should be revised to be tentatively ascribed to Val 213 or 217. These spectral changes in the carbonyl group of the amino acid residues in the transmembrane helices can be ascribed to modified hydrogen-bonding interactions as a result of an induced conformational change in these helices as compared with those of wild-type. In addition, deprotonation of Schiff base by raising pH from 7 to 10 resulted in the upfield displacement of the Val 49 peak by 0.45 ppm, and the latter two displaced unassigned signals indicated by the arrows were now completely suppressed by acquisition of fluctuational motions of the transmembrane helices under consideration in the time scale of 10^{-4} s, which might be interfered with magic angle spinning. At the same time, the Val 69 signal at the B−C loop was displaced upfield by 0.17 ppm.

In Figure 6, we compare ^{13}C CP-MAS (left) and DD-MAS (right) NMR spectra of D85N (A) at pH 10 with those of papain-cleaved D85N preparation (B). Now, it is possible to determine which ^{13}C NMR signals arose from Ala residues in the C-terminus. The four peaks labeled with arrows, at 15.61, 15.87, 16.88, and 17.90 ppm, in the former can be ascribed to the residues located at the C-terminus, as they are absent in the DD-MAS NMR spectrum of papain-cleaved preparation (right traces). Naturally, the intensity change of these peaks is less pronounced in the CP-MAS spectrum (left traces), because these residues seem to be too flexible to contribute to the CP-MAS NMR peaks, irrespective of the presence or absence of the C-terminus. In particular, the peak

Table 1: Summary of Amino-Acid Residues Involved in Characteristic Spectral Changes Induced for [3-^{13}C]Ala- and [1-^{13}C]Val-Labeled Proteins[a]

		α-helices				loop	
		B	transmembrane	D	G	B−C	E−F	F−G
	pH	Ala	Val	Ala	Ala	Val	Ala	Ala
D85N	10	39 (−)						
			49 (→)					
		51 (−)						
		53 (−)						
						69 (→)		
				126 (→)				
							160 (−)	
								196 (−)
					215 (−)			
D85N/D96N	10	39 (−)						
		51 (−)						
		53 (−)						
							160 (+)	
				126 (+)				
								196 (−)
					215 (−)			
Wild type	11			126 (−)				
								196 (−)
					215 (−)			

[a] (−) Suppressed peaks; (+) recovered peak after the peak-suppression; (→) displaced peak.

at 15.87 ppm (one or two Ala residues involved) was previously ascribed to the presence of an α-helical segment in the C-terminal protruding from membrane surface (*38*, *43*), consistent with a previous finding by fluorescence probe experiment (*54*). The peak position of the newly emerging peak at 15.61 ppm of D85N at alkaline pH (the uppermost peak indicated by the arrow) is consistent with that of Ala residues in the wild-type bR involved in the C-terminal α-helix as observed at lowered temperature below 10 °C (*43*). In addition, the lowermost peak from the C-terminal residues resonated at 17.90 ppm might be ascribed to Ala 235 in a turn-structure because of its neighbor to Pro residue (Figures 1 and 2).

DISCUSSION

Global Alteration of Conformation and Dynamics of the Protein Backbone Caused by Deprotonation of Schiff Base. It is found that global changes in the conformation and dynamics of the protein backbone by raising pH from 7 to 10 were visualized by ^{13}C NMR studies on [3-^{13}C]Ala- and [1-^{13}C]Val-labeled D85N and D85N/D96N mutants (Figures 2, 3, 5, and 6): they occurred as the result of the neutral Asn 85 and the deprotonation of Schiff base without illumination. In D85N, it was demonstrated that the side chain of Arg 82 is shifted toward the extracellular surface at neutral pH (*42*) and that the change remains in the M-like state at alkaline pH as well as M intermediate of WT (*55*). Characteristic spectral changes at pH 10 as viewed from the amino acid residues involved were also summarized in Table 1, utilizing three kinds of symbols: suppressed peaks (−), displaced peaks (→) and recovered peaks (+). To relate such observed spectral changes with their 3D structure so far revealed (*5*, *6*), we have located the labeled Ala (red) or Val (orange) residues in which their repective peaks were either suppressed or displaced, upon taking the M-like state, respectively, as shown in Figure 7. The E−F and F−G loops which acquired rapid motions in the M-like state were marked by the red strips. Spectral changes at pH 7 appear as displaced peaks of Ala 160 and 196 in the E−F and F−G loops instead of

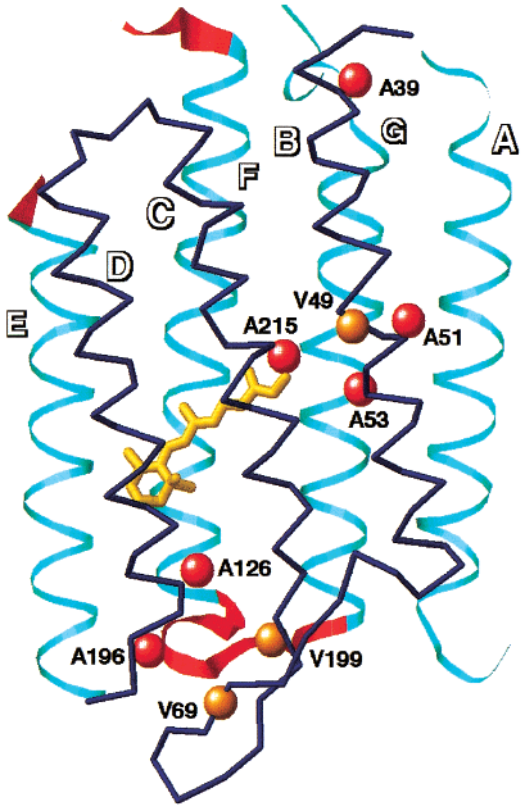

FIGURE 7: Schematic representation of 3D location of the Ala (red) or Val (orange) residues in bR (Luecke et al., refs *5* and *6*) in which respective peaks were either suppressed or displaced as a result of taking the M-like state, respectively. The E−F and F−G loops which acquired accelerated motions with correlation times in the order of 10^{-4} to 10^{-5} s in the M-like state were marked by the red strips.

the suppressed signals at pH 10. It is emphasized here that the ^{13}C chemical shifts of the loop region are time-averaged values undergoing conformational fluctuation among various preferred forms with time scale in the order of 10^{-4} s, as judged from the complete suppression of [2-^{13}C] or [1-^{13}C]-Ala-labeled wild-type and mutants due to failure of the peak-

narrowing by interference of such motional frequencies with proton decoupling and/or magic angle spinning (Yamaguchi et al., submitted for publication). These spectral changes were induced for equally both D85N and D85N/D96N, except for the absence of the spectral change at the extracelluar surface at Ala 126 and 196 in the latter, however.

It is expected that additional information as to conformational changes of backbone is available from the present ^{13}C NMR approach, if the current constraint of the "time scale" for the peak suppression (10^{-5} s) could be modified by recording ^{13}C NMR spectra of [1-^{13}C]Val-labeled proteins in which failure of the attempted "peak-narrowing" is ascribed to interference with magic angle spinning (10^{-4} s) rather than the proton decoupling frequency (10^{-5} s). As demonstrated and summarized in Figure 5 and Table 1, the downfield displacement of [1-^{13}C]Val-labeled signal of residue 49 of the helix B as well as the similar downfield displacement of the signals marked by the arrows (175.05 and 177.81 ppm) strongly indicate that at least one or two transmembrane α-helices were subject to the conformational change due to the single mutation at Asp 85 at neutral pH. It is more probable that these two peaks may arise from Val 213 or 217 of helix G, because they are located at the vicinity of Schiff base and Asp 212, although experimental confirmation based on preparation of site-directed mutants at these positions is under way in our laboratory. It is also pointed out that this change is specific to the color change from purple to blue as in R82Q, D212N, and R82Q/D212N (Tanio et al., manuscript in preparation). In addition, subsequent upfield displacement of the peaks for the Val 49 (B helix) and Val 69 (B−C loop) means a plausible involvement of the conformational rearrangement of the helix B by raising pH to form the M-like state in D85N. This finding is in favor of the intepretation by Kamikubo et al. (*21*) in which helices B and G are involved in large conformational changes in the M-state, although it is very difficult to argue about the involvement of F helix because there is no NMR data, at present, for N state. The peaks marked by the arrows, however, disappeared because of acquired motional freedom as described below. The resulting form is characteristic of the M state in view of the major structural change at the B and G helices of wild-type (*12*, *13*), although their 2D electron density maps of D85N are very similar to those of the MN state (*18*). Naturally, the acquisition of such motions in the transmembrane α-helices resulted in acquisition of more rapid motions of the cytoplasmic (and extracellular) loops, as judged from their suppressed peak intensities. The acquisition of such intermediate motion is consistent with the previously proposed destabilization of protein backbone interactions from loss of electrostatic interaction between the positively charged Schiff base and anionic residues as counterions (*30*), the resulting movement of the transmembrane helices detected by projection maps (*9*−*16*), and also by loss of electron density by single-crystal X-ray diffraction (*26*).

Consistent with a previous observation by FTIR measurement (*56*), very similar NMR spectral changes are noted in the transmembrane helical regions of bacterio-opsin (bO), as a result of acquisition of intermediate frequency motion due to removal of retinal (*44*). In fact, many common spectral features were observed at the transmembrane α-helices and featureless peaks in the high-field region except for the peak at 14.70 ppm. It appears that Ala 53 and 215 might be suppressed when retinal is removed as encountered for bO, due to their locations close to the Schiff base and Ala 84 and 39 might be also affected because of relaxed interaction between the Schiff base and Asp 85 (*44*). This might happen also in the present M-like state caused by deprotonation of Schiff base as described above. In fact, it was shown that a conformational change is produced both when constraints from the protonated Schiff base is relaxed in D85N mutant at higher pH (*18*, *30*) and when removed permanently in bO (*56*).

In a recent paper by X-ray diffraction on the structure of MN intermediate, it is reported that the hinge is definitely not at Tyr 185 (where the helix does not move) but located much more to the cytoplasmic side (*26*). This favors the idea that the E−F loop plays a large role in the tilt, because this loop becomes very flexible during the M-like state. It should be also taken into account, however, that the present data based on 2D crystal is not always the same as that of 3D crystal, at least as surface residues are concerned in view of the recent comparative evaluation of the data by cryo-electron microscope, X-ray diffraction, and AFM measurement (*57*). It is mentioned that acquisition of such motions both in the transmembrane helices and loop(s) with correlation times of 10^{-5} s as compared with correlation time of loop motion in the order of 10^{-4} s under physiological condition (Yamaguchi et al., submitted for publication) is essential to complete the conformational switch during M-state in view of overall lifetime of 1 ms in this state. It seems inevitable, however, that the presence of such motion at ambient temperature could be sensed as disordered structure at lower temperature. Further, there appears to be a distinct spectral change between the M-like states in D85N (Figure 2C) and D85N/D96N (Figure 3C), despite their similarity by X-ray diffraction (*18*, *30*). In particular, it appears that flexibility at the extracellular side of D85N acquired upon assuming the M-like state is strongly inhibited by the absence of charge at Asn 96 in the double mutant (see Figures 2 and 3).

Interaction of the C-Terminal Helix and Loops. The most intense peak in the CP-MAS NMR spectra of D85N and D85N/D96N resonated at 15.8−15.9 ppm remains unchanged throughout pH ranges studied here. It can be ascribed to Ala 228 or 233 assuming that a short α-helical segment protrudes from the membrane surface (*38*, *43*, *44*), although this helix has not yet been identified by diffraction studies mentioned above nor by heavy-atom labeling experiment (*33*). It appears, however, that direct observation of this helix is difficult because of the 3D crystallographic contacts (*57*) which may interfere with formation of surface structure of cytoplasmic side, consisting of the C-terminal helix complexed with E−F and C−D loops through a mechanism as will be described below. The physiological significance of such α-helical segment has not yet been clarified. Very recently, we proposed, based on data from a variety of site-directed mutants at the cytoplasmic sides and preparations of papain- or pronase-treated bR, that this C-terminal α-helix is linked with cytoplasmic loops which undergo conformational fluctuations with correlation times in the order of 10^{-4} s (Yamaguchi et al., submitted for publication), to form cytoplasmic surface structure through salt bridges among them. The presence of such a (globular) structure protruding from the membrane surface was previously implied by

fluorescence probe experiments (*54*) and also by recent observations by atomic force microscope (AFM) (*57, 58*).

In this connection, it is interesting to note that the conformation and dynamics of the C-terminal helix and its vicinity protruding from the membrane surface in the M-like state are strongly affected by the ionization state of both residue 85 and the Schiff base located within the transmembrane helices, as demonstrated in the ^{13}C NMR spectra in Figure 2. This is not surprising because the C-terminal helix is strongly coupled with motional state of the E−F loop undergoing rapid reorientational motions caused by deprotonation of the Schiff base. Alternatively, the reorganized helix G in the M state (*34*) may modify the interaction between the C-terminal helix and loops, which in turn can be monitored as a change of the stability of the C-terminal α-helix. In particular, the peak at 15.61 ppm, which is absent in the wild-type and in D85N at neutral pH but significant in this mutant at higher pH, can be ascribed to one of the residues in the C-terminal α-helix either Ala 228 or 233, because this peak was previously attributed to the presence of more stabilized C-terminal α-helix of wild-type at low temperature (0 °C). Naturally, the altered conformation and dynamics of the cytoplasmic E−F loops in the M-like state, as demonstrated by the suppressed peak-intensities due to the onset of intermediate frequency (see also Figure 7), may result in conformational changes of the above-mentioned C-terminal α-helix through specific interaction between the looped structure and the C-terminal α-helix, as proposed already.

Long-Distance Effects of Neutralization of Asp 96 toward Conformational Changes at the Extracellular Side. It is interesting to note that neutralization of Asp 96 in D85N/D96N mutant inhibited the increased flexibility of the F−G loop through partial restriction of the movement of the transmembrane helices, F or G, and conformational change at the helix D in the extracellular side of D85N mutant at pH 10, in [3-^{13}C]Ala-labeled proteins. It is likely that this sort of restriction might be caused by the presence of deprotonated Asp 96 in D85N at pH 10. This state may be modified by D85N/D96N mutant, however. Therefore, deprotonation of Asp 96 at D85N modifies the conformation of the extracellular side via the presence of plausible long distance interaction between the residues located at the both sides. The existence of such long distance interactions such as D85-V49-T46-D96 and D85-E204 has been previously proposed and partly experimentally confirmed (*41*, *42*, *59*−*62*) as interactions among the backbone and side chains of the concerned residues or a hydrogen bond network with water molecules. The most probable explanation in this case may be a lowered pK_a for Asp 96 under the influence of the protonated state of Asp 85. To prove this view, a detailed pH-titration study for ^{13}C NMR measurements of [1-^{13}C]-Val-labeled mutants is under way in our laboratory. In this connection, it was pointed out recently that the high pK_a of Asp 96 drops to 7.1 during the lifetime of the N intermediate (*63*).

CONCLUDING REMARKS

We have demonstrated that our ^{13}C NMR approach is able to locate the domain that undergoes conformational changes, as well as changes in dynamics, in the M-like state of bR at ambient temperature which would be of biological significance. In particular, it is emphasized that the present NMR approach is the only means to be able to clarify such dynamic aspect of protein backbone under physiological condition. In fact, the present NMR approach is based on the fact that the well-resolved signals are available from successful "peak-narrowing" procedure by the CP-MAS experiment, as encountered for wild-type and a variety of site-directed mutants of bR, in which the observed NMR signals arose from inhomogeneously broadened signals at *ambient temperature*. Such attempt, however, could be unsuccessful, if the observed signals of certain residues were homogeneously broadened due to failure of the peak-narrowing as a result of interference of incoherent frequency of internal motions, if any, with coherent frequencies of proton decoupling or magic angle spinning, as discussed in the text.

This approach is a completely nonperturbing technique and suitable for the study of the conformation and dynamics of interfacial residues which are difficult to be examined by diffraction methods. The observed acquisition of greater flexibility as demonstrated as the time-averaged structures of the F−G or E−F loops in the M-like state may also play an important role in the movement of the transmembrane helices in the photocycle also, although such flexibility in the extracellular side is strongly influenced by the ionization state of Asp 96. Finally, it is worthwhile to point out that different kinds of pictures are now available for conformation and/or dynamics of bacteriorhodopsin from measurements by X-ray diffraction, FTIR, and NMR: X-ray diffraction gives rise to time-averaged structures, while FTIR can detect the change in vibration modes of picosecond time scale, which would be corresponding to the conformational change. However, FTIR itself does not give any information on the rate constant of such conformational change. Dynamic pictures with various time scales can be selectively detected by this kind of high-resolution solid-state NMR at ambient temperature. In particular, the presence of intermediate motions with time scales of milli- or microseconds could be detected by observation of suppressed peak intensities as a result of failure of attempted peak narrowing by solid-state NMR, as demonstrated in this paper. It is emphasized that the major conformational changes accompanied by formation of M-state (or M-like state) as detected by the X-ray diffraction studies were made possible by the presence of such large-amplitude, intermediate motions of the transmembrane α-helices and the interhelical loops as discussed in this paper.

This approach is therefore potentially useful for clarification of the molecular mechanism of signal transduction for a variety of G-protein coupled receptors.

REFERENCES

1. Grigorieff, N., Ceska, T. A., Downing, K. H., Baldwin, J. M., and Henderson, R. (1996) *J. Mol. Biol. 259*, 393−421.
2. Kimura, Y., Vassylyev, D. G., Miyazawa, A., Kidera, A., Matsushima, M., Mitsuoka, K., Murata, K., Hirai, T., and Fujiyoshi, Y. (1997) *Nature 389*, 206−211.
3. Mitsuoka, K., Hirai, T., Murata, K., Miyazawa, A., Kidera, A., Kimura, Y., and Fujiyoshi, Y. (1999) *J. Mol. Biol. 286*, 861−882.
4. Pebay-Peyroula, E., Rummel, G., Rosenbusch, J. P., and Landau, E. M. (1997) *Science 277*, 1676−1681.

5. Luecke, H., Richter, H. T., and Lanyi, J. K. (1998) *Science 280*, 1934−1937.
6. Luecke, H., Schobert, B., Richter, H. T., Cartailler, J. P., and Lanyi, J. K. (1999) *J. Mol. Biol. 291*, 899−911.
7. Essen, L. O., Siegert, R., Lehmann, W. D., and Oesterhelt, D. (1998) *Proc. Natl. Acad. Sci. U.S.A. 95*, 11673−11678.
8. Belrhali, H., Nollert, P., Royant, A., Menzel, C., Rosenbusch, J. P., Landau, E. M., and Pebay-Peyroula, E. (1999) *Struct. Folding Des. 7*, 909−917.
9. Dencher, N. A., Dresselhaus, D., Zaccai, G., and Büldt, G. (1989) *Proc. Natl. Acad. Sci. U.S.A. 86*, 7876−7879.
10. Hauss, T., Büldt, G., Heyn, M. P., and Dencher, N. A. (1994) *Proc. Natl Acad. Sci. U.S.A. 91*, 11854−11858.
11. Koch, M. H., Dencher, N. A., Oesterhelt, D., Plohn, H. J., Rapp, G., and Büldt, G. (1991) *EMBO J. 10*, 521−526.
12. Nakasako, M., Kataoka, M., Amemiya, Y., and Tokunaga, F. (1991) *FEBS Lett. 292*, 73−75.
13. Kamikubo, H., Kataoka, M., Varo, G., Oka, T., Tokunaga, F., Needleman, R., and Lanyi, J. K. (1996) *Proc. Natl. Acad. Sci. U.S.A. 93*, 1386-1390.
14. Sass, H. J., Schachowa, I. W., Rapp, G., Koch, M. H., Oesterhelt, D., Dencher, N. A., and Büldt, G. (1997) *EMBO J. 16*, 1484−1491.
15. Subramaniam, S., Gerstein, M., Oesterhelt, D., and Henderson, R. (1993) *EMBO J. 12*, 1−8.
16. Subramaniam, S., Lindahl, M., Bullough, P., Faruqi, A. R., Tittor, J., Oesterhelt, D., Brown, L., Lanyi, J., and Henderson, R. (1999) *J. Mol. Biol. 287*, 145−161.
17. Vonck, J. (1996) *Biochemistry 35*, 5870−5878.
18. Kataoka, M., Kamikubo, H., Tokunaga, F., Brown, L. S., Yamazaki, Y., Maeda, A., Sheves, M., Needleman, R., and Lanyi, J. K. (1994) *J. Mol. Biol. 243*, 621−638.
19. Lanyi, J. K. (1995) *Nature 375*, 461−463.
20. Lanyi, J. K. (1997) *J. Biol. Chem. 272*, 31209−31212.
21. Kamikubo, H., Oka, T., Imamoto, Y., Tokunaga, F., Lanyi, J. K., and Kataoka, M. (1997) *Biochemistry 36*, 12282−12287.
22. Thorgeirsson, T. E., Xiao, W., Brown, L. S., Needleman, R., Lanyi, J. K., and Shin, Y. K. (1997) *J. Mol. Biol. 273*, 951−957.
23. Steinhoff, H. J., Mollaaghababa, R., Altenbach, C., Hideg, K., Krebs, M., Khorana, H. G., and Hubbell, W. L. (1994) *Science 266*, 105−107.
24. Rink, T., Riesle, J., Oesterhelt, D., Gerwert, K., and Steinhoff, H. J. (1997) *Biophys. J. 73*, 983−993.
25. Pfeiffer, M., Rink, T., Gerwert, K., Oesterhelt, D., and Steinhoff, H. J. (1999) *J. Mol. Biol. 287*, 163−171.
26. Luecke, H., Schobert, B., Richter, H. T., Cartailler, J. P., and Lanyi, J. K. (1999) *Science 286*, 255−261.
27. Ormos, P. (1991) *Proc. Natl. Acad. Sci. U.S.A. 88*, 473−477.
28. Nilsson, A., Rath, P., Olejnik, J., Coleman, M., and Rothschild, K. J. (1995) *J. Biol.Chem. 270*, 29746−29751.
29. Turner, G. J., Miercke, L. J., Thorgeirsson, T. E., Kliger, D. S., Betlach, M. C., and Stroud, R. M. (1993) *Biochemistry 32*, 1332−1337.
30. Brown, L. S., Kamikubo, H., Zimanyi, L., Kataoka, M., Tokunaga, F., Verdegem, P., Lugtenburg, J., and Lanyi, J. K. (1997) *Proc. Natl. Acad. Sci. U.S.A. 94*, 5040−5044.
31. Brown, L. S., Dioumaev, A. K., Needleman, R., and Lanyi, J. K. (1998) *Biochemistry 37*, 3982−3993.
32. Krebs, M. P., and Khorana, H. G. (1993) *J. Bacteriol. 175*, 1555−1560.
33. Behrens, W., Alexiev, U., Mollaaghababa, R., Khorana, H. G., and Heyn, M. P. (1998) *Biochemistry 37*, 10411−10419.
34. Oka, T., Kamikubo, H., Tokunaga, F., Lanyi, J. K., Needleman, R., and Kataoka, M. (1999) *Biophys. J. 76*, 1018−1023.
35. Tuzi, S., Naito, A., and Saitô, H. (1993) *Eur. J. Biochem. 218*, 837−844.
36. Tuzi, S., Naito, A., and Saitô, H. (1994) *Biochemistry 33*, 15046−15052.
37. Tuzi, S., Naito, A., and Saitô, H. (1996) *Eur. J. Biochem. 239*, 294−301.
38. Tuzi, S., Yamaguchi, S., Naito, A., Needleman, R., Lanyi, J. K., and Saitô, H. (1996) *Biochemistry 35*, 7520−7527.
39. Tuzi, S., Yamaguchi, S., Tanio, M., Konishi, H., Inoue, S., Naito, A., Needleman, R., Lanyi, J. K., and Saitô, H. (1999) *Biophys. J. 76*, 1523−1531.
40. Tanio, M., Tuzi, S., Yamaguchi, S., Konishi, H., Naito, A., Needleman, R., Lanyi, J. K., and Saitô, H. (1998) *Biochim. Biophys. Acta 1375*, 84−92.
41. Tanio, M., Inoue, S., Yokota, K., Seki, T., Tuzi, S., Needleman, R., Lanyi, J. K., Naito, A., and Saitô, H. (1999) *Biophys. J. 77*, 431−442.
42. Tanio, M., Tuzi, S., Yamaguchi, S., Kawaminami, R., Naito, A., Needleman, R., Lanyi, J. K., and Saitô, H. (1999) *Biophys. J. 77*, 1577−1584.
43. Yamaguchi, S., Tuzi, S., Seki, T., Tanio, M., Needleman, R., Lanyi, J. K., Naito, A., and Saitô, H. (1998) *J. Biochem. (Tokyo) 123*, 78−86.
44. Yamaguchi, S., Tuzi, S., Tanio, M., Naito, A., Lanyi, J. K., Needleman, R., and Saitô, H. (2000) *J. Biochem. (Tokyo) 127*, 861−869.
45. Saitô, H., Tuzi, S., Yamaguchi, S., Tanio, M., and Naito, A. (2000) *Biochim. Biophys. Acta 1460*, 39−47.
46. Saitô, H. (1986) *Magn. Reson. Chem. 24*, 835−852.
47. Saitô, H., and Ando, I. (1989) *Annu. Rep. NMR Spectrosc. 21*, 209−290.
48. Saitô, H., Tuzi, S., and Naito, A. (1998) *Annu. Rep. NMR Spectrosc. 36*, 79−121.
49. Mehring, M. (1983) *Principles of High-Resolution NMR in Solids*, 2nd ed., Springer.
50. Rothwell, W. P., and Waugh, J. S. (1981) *J. Chem. Phys. 74*, 2721−2732.
51. Onishi, H., McCance, E. M., and Gibbons, N. E. (1965) *Can. J. Microbiol. 11*, 365−373.
52. Oesterhelt, D., and Stoeckenius, W. (1974) *Methods. Enzymol. 31*, 667−678.
53. Liao, M. J., and Khorana, H. G. (1984) *J. Biol. Chem. 259*, 4194−4199.
54. Renthal, R., Dawson, N., Tuley, J., and Horowitz, P. (1983) *Biochemistry 22*, 5−12.
55. Petkova, A. T., Hu, J. G., Bizounok, M., Simpson, M., Griffin, R. G., and Herzfeld, J. (1999) *Biochemistry 38*, 1562−1572.
56. Ludlam, G. J., and Rothschild, K. J. (1997) *FEBS Lett. 407*, 285−288.
57. Heymann, J. B., Müller, D. J., Landau, E. M., Rosenbusch, J. P., Pebay-Peyroula, E., Büldt, G., and Engel, A. (1999) *J. Struct. Biol. 128*, 243−249.
58. Müller, D. J., Sass, H. J., Müller, S. A., Büldt, G., and Engel, A. (1999) *J. Mol. Biol. 285*, 1903−1909.
59. Brown, L. S., Yamazaki, Y., Maeda, A., Sun, L., Needleman, R., and Lanyi, J. K. (1994) *J. Mol. Biol. 239*, 401−414.
60. Yamazaki, Y., Hatanaka, M., Kandori, H., Sasaki, J., Karstens, W. F., Raap, J., Lugtenburg, J., Bizounok, M., Herzfeld, J., Needleman, R., Lanyi, J. K., and Maeda, A. (1995) *Biochemistry 34*, 7088−7093.
61. Yamazaki, Y., Tuzi, S., Saitô, H., Kandori, H., Needleman, R., Lanyi, J. K., and Maeda, A. (1996) *Biochemistry 35*, 4063−4068.
62. Yamazaki, Y., Kandori, H., Needleman, R., Lanyi, J. K., and Maeda, A. (1998) *Biochemistry 37*, 1559−1564.
63. Zscherp, C., Schlesinger, R., Tittor, J., Oesterhelt, D., and Heberle, J. (1999) *Proc. Natl. Acad. Sci. U.S.A. 96*, 5498−5503.

BI0015820